Journal of Magnetism and Magnetic Materials 442 (2017) 270–278

Contents lists available at ScienceDirect

Journal of Magnetism and Magnetic Materials

journal homepage: www.elsevier.com/locate/jmmm

Research articles

Numerical simulation of magnetic convection ferrofluid flow in a permanent magnet–inserted cavity

Majid Ashouri, Mohammad Behshad Shafii *

School of Mechanical Engineering, Sharif University of Technology, Tehran, Iran

ARTICLE INFO

Article history:
Received 26 November 2016
Received in revised form 17 April 2017
Accepted 16 June 2017
Available online 19 June 2017

Keywords:
Ferrofluid
Magnetic convection
Nusselt number
Square cavity
Thermomagnetic

ABSTRACT

The magnetic convection heat transfer in an obstructed two-dimensional square cavity is investigated numerically. The walls of the cavity are heated with different constant temperatures at two sides, and isolated at two other sides. The cavity is filled with a high Prandtl number ferrofluid. The convective force is induced by a magnetic field gradient of a thermally insulated square permanent magnet located at the center of the cavity. The results are presented in the forms of streamlines, isotherms, and Nusselt number for various values of magnetic Rayleigh numbers and permanent magnet size. Two major circulations are generated in the cavity, clockwise flow in the upper half and counterclockwise in the lower half. In addition, strong circulations are observed around the edges of the permanent magnet surface. The strength of the circulations increase monotonically with the magnetic Rayleigh number. The circulations also increase with the permanent magnet size, but eventually, are suppressed for larger sizes. It is found that there is an optimum size for the permanent magnet due to the contrary effects of the increase in magnetic force and the increase in flow resistance by increasing the size. By increasing the magnetic Rayleigh number or isothermal walls temperature ratio, the heat transfer rate increases.

1. Introduction

Ferrofluids, colloidal suspensions of ferromagnetic nanoparticles, have special performances under the influence of magnetic fields [1]. Applications mainly take advantage of the control by magnetic forces over ferrofluid physical and flowing properties. The mechanical applications of ferrofluids include heat transfer and damping in loud speakers [2,3], lubricants and seals [4,5], sensors [6–9], thermomagnetic pumps [10,11], heat pipes [12,13], ferrohydrodynamic pumps [14,15], microfluidic pumps and valves [16–18], mixing [19,20], magnetowetting [21,22], and magnetic manipulation [23,24]. Review papers have discussed the microscale interactions between magnetism and fluid flow for controlling fluidic functions [25] and mechanical applications of micromagnetofluidics [26,27]. Moreover, the use of ferrofluids as heat transfer fluids is attractive in many engineering applications since the heat transfer rate and fluid flow can be controlled by external magnetic fields [28].

The magnetic fields suppress the flow of electrically conducting fluids due to the magnetohydrodynamic (MHD) effects. This phenomenon is widely used to control the flow and heat transfer processes of liquid metals [29]. Subsequently, MHD can mitigate or neutralize the development of flow instabilities [30,31]. In contrast, flow and heat transfer of magnetic fluids can either be enhanced or interrupted under the effect of applied magnetic fields. As a result, in a magnetized ferrofluid with a non-uniform temperature distribution, an interesting continuous convection occurs. This phenomenon, which is called the *magnetic convection*, is the result of magnetization differences in the ferrofluid occurring due to temperature gradients. The performance of small-scale cooling devices can be enhanced by using magnetic convection of ferrofluids, whereas the heat transfer rate can be greater than the ordinary natural convection [32]. Also, magnetic convection enhances the heat transfer process in microgravity condition [33].

The magnetic convection has been widely investigated experimentally and numerically confirming its effect in augmentation of heat transfer rate as reviewed in [28,34]. The magnetic convection around cylinders immersed in ferrofluids exposed to the magnetic fields is studied in [35,36]. The forced convection flows of ferrofluid under the influence of magnetic fields are reported for rectangular channels [37,38], tube [39], and vented cavity [40]. The magnetic convection of ferrofluids in enclosures is investigated for different geometries: in a rectangular Hele-Shaw cell [41], cylinder [42,43], semi annulus enclosure [44,45], triangular cavity [46], cubic cavities [47,48], narrow rectangular cavity [49], and in

* Corresponding author.
E-mail addresses: ashouri_majid@mech.sharif.edu (M. Ashouri), behshad@sharif.edu (M. Behshad Shafii).

http://dx.doi.org/10.1016/j.jmmm.2017.06.089
0304-8853/

Nomenclature

Symbol and Property

B_r	Residual magnetization of permanent magnet
c	Specific heat
d	Size of the permanent magnet
D	Size of the cavity
H	Magnetic field strength
k	Thermal conductivity
k_B	Boltzmann constant
M	Magnetization
M_d	Magnetic nanoparticle magnetization
M_s	Saturation magnetization
Nu	Nusselt number
$\overline{\text{Nu}}$	Overall Nusselt number
P	Pressure
Pr	Prandtl number
Ra_m	Magnetic Rayleigh number
T	Temperature
t_r	Temperature ratio
u, v	Velocity components
$\mathbf{V}$	Velocity vector
V_p	Magnetic nanoparticle average volume
x, y	Cartesian coordinates

Greek symbols

α	Thermal diffusivity
β	Magnetization coefficient
β_c	Magnetization coefficient at reference temperature
μ_0	Magnetic permeability of free space
μ	Dynamic viscosity
ρ	Fluid density
ϕ	Magnetic nanoparticle volume fraction

Subscripts

c, R	Cold (right) wall
h, L	Hot (left) wall

Superscripts

$*$	Non-dimensional form

square cavities [50–59]. The effect of magnetic field on the natural convection of a magnetic fluid in a bottom-heated square cavity with insulated side walls was studied by Yamaguchi et al. [51,52]. The performed numerical analysis confirmed their experimental results showing a destabilizing effect on the flow transition by applying the magnetic field. Scaling analysis and numerical correlation for magnetic convection in the absence of buoyancy convection have been reported in Refs. [53] and [54], respectively. In a detailed numerical model, the influence of a uniform magnetic field on natural convection in a square cavity was investigated by Krakov and Nikiforov [55]. They disclosed that the geometry of the cavity filled with magnetic fluid and temperature dependence of fluid magnetization have influences on the magnetic field distribution in the cavity and hence the outer uniform magnetic field becomes nonuniform. Other studies included the thermal and magnetic convection ferrofluid flow in a partitioned cavity [56], a porous cavity [57], a partially heated cavity [58], and a corrugated cavity [59].

In the present study, flow and heat transfer characteristics of magnetic convection in a ferrofluid filled square cavity is studied numerically. The magnetic force is produced by a square permanent magnet located at the center of the cavity, while the buoyancy force is absent. The effect of permanent magnet size at different magnetic Rayleigh numbers on the flow and heat transfer rate is investigated. While increasing the permanent magnet size has the positive effect of strengthening the ferrofluid driving force, however it has the unfavorable effect of increasing the resistance to the fluid flow; thus, the optimal permanent magnet size for best heat transfer rate is studied.

2. Mathematical formulation

The problem is schematically shown in Fig. 1, which considers a two-dimensional square cavity of width D filled with a ferrofluid. The top and bottom walls of the cavity are adiabatic and the left and right vertical walls are kept at constant temperatures T_h and T_c, respectively. A square permanent magnet of poles distance d is inserted into the center of the cavity. The surfaces of the permanent magnet are adiabatic. The thermomagnetic convection occurs due to the combined effect of magnetic field and temperature gradient on the ferrofluid. The flow is considered laminar, incompressible and two dimensional. The thermal properties are assumed to be constant. The governing conservation equations can be written as [60]

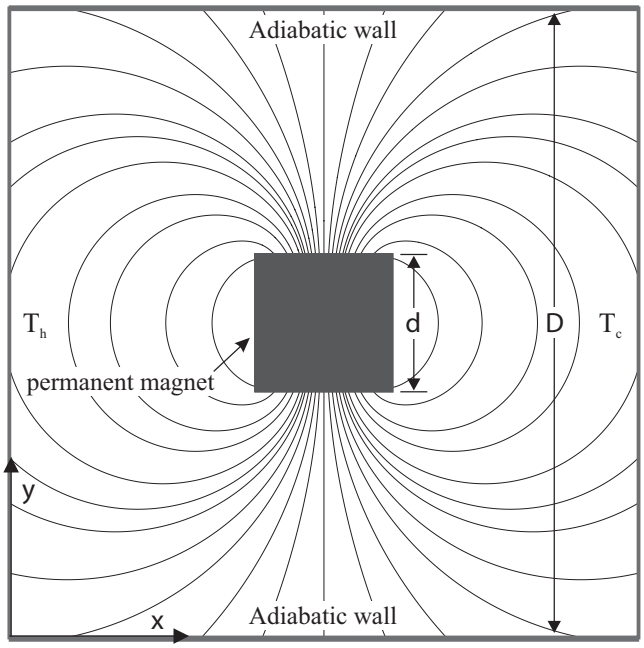

Fig. 1. Schematic of the problem geometry. The magnetic field lines are plotted for a permanent magnet with the poles facing the adiabatic walls.

$$\nabla.\mathbf{V} = 0 \tag{1}$$

$$\rho\mathbf{V}.\nabla\mathbf{V} = -\nabla P + \mu\nabla^2\mathbf{V} + \mu_0(\mathbf{M}.\nabla)\mathbf{H} \tag{2}$$

$$\rho c\mathbf{V}.\nabla T = k\nabla^2 T - \mu_0 T\frac{\partial \mathbf{M}}{\partial T}(\mathbf{V}.\nabla)\mathbf{H} \tag{3}$$

where ρ, μ, c, and k are the density, viscosity, specific heat, and thermal conductivity of the ferrofluid, respectively. The term $\mu_0(\mathbf{M}.\nabla)\mathbf{H}$ in the momentum equation represents the Kelvin mag-

netic force, and the similar added term in the energy equation indicates heating due to magnetization. In these expressions, μ_0 is the free-space permeability, **M** is the ferrofluid magnetization vector, and **H** is the magnetic field intensity vector. The direction of magnetization of ferrofluid is always in the direction of the local magnetic field [60]; thus, the magnetic body force can be rewritten as

$$\mu_0(\mathbf{M}.\nabla)\mathbf{H} = \mu_0\frac{M}{H}(\mathbf{H}.\nabla)\mathbf{H} = \mu_0\frac{M}{H}\left[\frac{1}{2}\nabla(\mathbf{H}.\mathbf{H}) - \mathbf{H}\times(\nabla\times\mathbf{H})\right] \quad (4)$$

If we neglect the displacement current produced by the ferrofluid movement (i.e., $\nabla\times\mathbf{H}=0$), then by $1/2\nabla(\mathbf{H}.\mathbf{H}) = H\nabla H$ the magnetic body force can be expressed as $\mu_0 M\nabla H$ where H is the magnitude of the magnetic field. The resulting expression reveals that for the non-electric conductive medium, if the square permanent magnet of Fig. 1 is rotated 90 degrees (i.e., the poles face the isothermal walls), the magnetic force remains unchanged. On the other hand, thermomagnetic heating has a little effect on the problem being investigated and can be ignored [54]. The governing equations in the non-dimensional form can be expressed as Eqs. (5)–(8).

$$\frac{\partial u^*}{\partial x^*} + \frac{\partial v^*}{\partial y^*} = 0 \quad (5)$$

$$u^*\frac{\partial u^*}{\partial x^*} + v^*\frac{\partial u^*}{\partial y^*} = -\frac{\partial P^*}{\partial x^*} + \mathrm{Pr}\left(\frac{\partial^2 u^*}{\partial x^{*2}} + \frac{\partial^2 u^*}{\partial y^{*2}}\right) + \mathrm{PrRa}_m\frac{M^*}{H^*}\left(H_x^*\frac{\partial H_x^*}{\partial x^*} + H_y^*\frac{\partial H_y^*}{\partial x^*}\right) \quad (6)$$

$$u^*\frac{\partial v^*}{\partial x^*} + v^*\frac{\partial v^*}{\partial y^*} = -\frac{\partial P^*}{\partial y^*} + \mathrm{Pr}\left(\frac{\partial^2 v^*}{\partial x^{*2}} + \frac{\partial^2 v^*}{\partial y^{*2}}\right) + \mathrm{PrRa}_m\frac{M^*}{H^*}\left(H_x^*\frac{\partial H_x^*}{\partial y^*} + H_y^*\frac{\partial H_y^*}{\partial y^*}\right) \quad (7)$$

$$u^*\frac{\partial T^*}{\partial x^*} + v^*\frac{\partial T^*}{\partial y^*} = \left(\frac{\partial^2 T^*}{\partial x^{*2}} + \frac{\partial^2 T^*}{\partial y^{*2}}\right) \quad (8)$$

The non-dimensional variables in the above equations have been defined as $x^* = x/D$, $y^* = y/D$, $u^* = u/(\alpha/D)$, $v^* = v/(\alpha/D)$, $P^* = P/(\rho\alpha^2/D^2)$, $T^* = (T-T_c)/(T_h-T_c)$, $M^* = M/M_s$, $H^* = H/(B_r/\mu_0)$, where $\alpha = k/(\rho c)$ is the thermal diffusivity of ferrofluid, M_s is the saturation magnetization of ferrofluid, and B_r is the residual magnetization of permanent magnet. The Prandtl number and Magnetic Rayleigh number are defined as

$$Pr = \frac{\mu c}{k}, \quad \mathrm{Ra}_m = \frac{B_r M_s D^2}{\mu\alpha} \quad (9)$$

Ferrofluid equilibrium magnetization is given by the Langevin equation for paramagnetism [61] as

$$M^* = \coth\beta H^* - \frac{1}{\beta H^*}, \quad \beta = \frac{\beta_c}{1+t_r T^*}, \quad (10)$$

The two dimensionless parameters β_c and t_r are defined as

$$\beta_c = \frac{B_r M_s}{N k_B T_c} = \frac{B_r M_d V_p}{k_B T_c}, \quad t_r = \frac{T_h - T_c}{T_c} \quad (11)$$

where $M_s = M_d\phi$ is the saturation magnetization of ferrofluid with magnetic nanoparticles volume fraction of ϕ and magnetization of M_d; k_B is the Boltzmann constant, N is the number of magnetic dipoles per unit volume, i.e. $N = \phi/V_p$ where $V_p = \pi d_p^3/6$ is the volume of a magnetic nanoparticle with diameter of d_p.

To calculate the magnetic field strength for the square permanent magnets used in this study, it is assumed that the magnetic permeability does not vary in the domain (the effect of ferromagnetic material is ignored). Based on this simplification, the magnetic field strength due to the magnetic dipole in the x and y directions (in the coordinates of Fig. 1) for a two-dimensional permanent magnet is expressed as Eqs. (12) and (13) [54],

$$H_x^* = \frac{1}{4\pi}\left\{\ln\left[1+\frac{\left(x^*-\frac{1-d^*}{2}\right)^2}{\left(y^*-\frac{1+d^*}{2}\right)^2}\right] - \ln\left[1+\frac{\left(x^*-\frac{1+d^*}{2}\right)^2}{\left(y^*-\frac{1+d^*}{2}\right)^2}\right] + \ln\left[1+\frac{\left(x^*-\frac{1+d^*}{2}\right)^2}{\left(y^*-\frac{1-d^*}{2}\right)^2}\right] - \ln\left[1+\frac{\left(x^*-\frac{1-d^*}{2}\right)^2}{\left(y^*-\frac{1-d^*}{2}\right)^2}\right]\right\} \quad (12)$$

$$H_y^* = \frac{1}{2\pi}\left\{\arctan\left[\frac{x^*-\frac{1-d^*}{2}}{y^*-\frac{1+d^*}{2}}\right] - \arctan\left[\frac{x^*-\frac{1+d^*}{2}}{y^*-\frac{1+d^*}{2}}\right] + \arctan\left[\frac{x^*-\frac{1+d^*}{2}}{y^*-\frac{1-d^*}{2}}\right] - \arctan\left[\frac{x^*-\frac{1-d^*}{2}}{y^*-\frac{1-d^*}{2}}\right]\right\} \quad (13)$$

where $d^* = d/D$. Partial derivatives of these components, appeared in Eqs. (6) and (7), are calculated analytically.

The hydrodynamic and the thermal boundary conditions are specified in Eqs. (14) and (15), respectively.

$$u^* = 0 \text{ and } v^* = 0 (\text{for all walls}) \quad (14)$$

$$T^* = 1(\text{on left wall}), \quad T^* = 0(\text{on right wall})$$
$$\partial T^*/\partial y^* = 0(\text{for other walls and permanent magnet surfaces}), \quad (15)$$

The local and average Nusselt numbers are defined as

$$\mathrm{Nu}_{L/R} = \left|\frac{\partial T^*}{\partial x^*}\right|_{x^*=0/1}, \quad \overline{\mathrm{Nu}} = \int_0^1 \left|\frac{\partial T^*}{\partial x^*}\right|_{x^*=0} dy^* \quad (16)$$

3. Numerical method

The coupled governing equations were transformed into algebraic equations using the finite volume method. Second order upwind scheme was utilized to discretize the momentum and energy equations. The SIMPLE (Semi-Implicit for Pressure Linked Equations) algorithm [62] was used to handle the pressure–velocity coupling.

Numerical solutions were carried out at uniform grid sizes of 0.001 for $\mathrm{Ra}_m \geqslant 1\times10^9$ and 0.002 for lower magnetic Rayleigh numbers. The results of average Nusselt number for different grid

Table 1
Comparison of the average Nusselt number for different grid sizes (Pr = 1000, $\beta_c = 60$, $d^* = 0.5$, and $t_r = 0.2$); the values in parentheses are the relative errors.

Grid size	$\mathrm{Ra_m} = 2.5\times10^8$	$\mathrm{Ra_m} = 1\times10^9$	$\mathrm{Ra_m} = 5\times10^9$
0.005	6.153 (4.64%)	9.550 (15.4%)	15.59 (34.6%)
0.002	5.904 (0.41%)	8.427 (1.85%)	12.20 (5.35%)
0.001	5.882 (0.03%)	8.258 (0.19%)	11.60 (0.17%)
0.0005	5.880	8.274	11.58

Table 2
Comparison of present results and previous results of average Nusselt number in an air-filled cavity for $\mathrm{Ra} = 10^5$.

d^*	k_r	[63]	[64]	Present
0	–	4.561	4.536	4.533
0.5	5.0	4.324	4.280	4.322
0.5	0.2	4.624	4.605	4.626

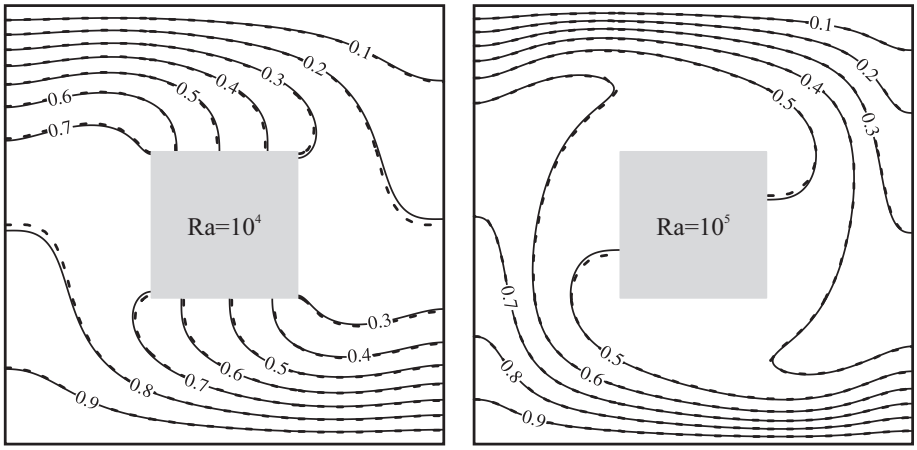

Fig. 2. Comparison of present results (solid lines) and previous results (dashed lines) of isotherms in an air-filled cavity containing an adiabatic block of size $d^* = 1/3$.

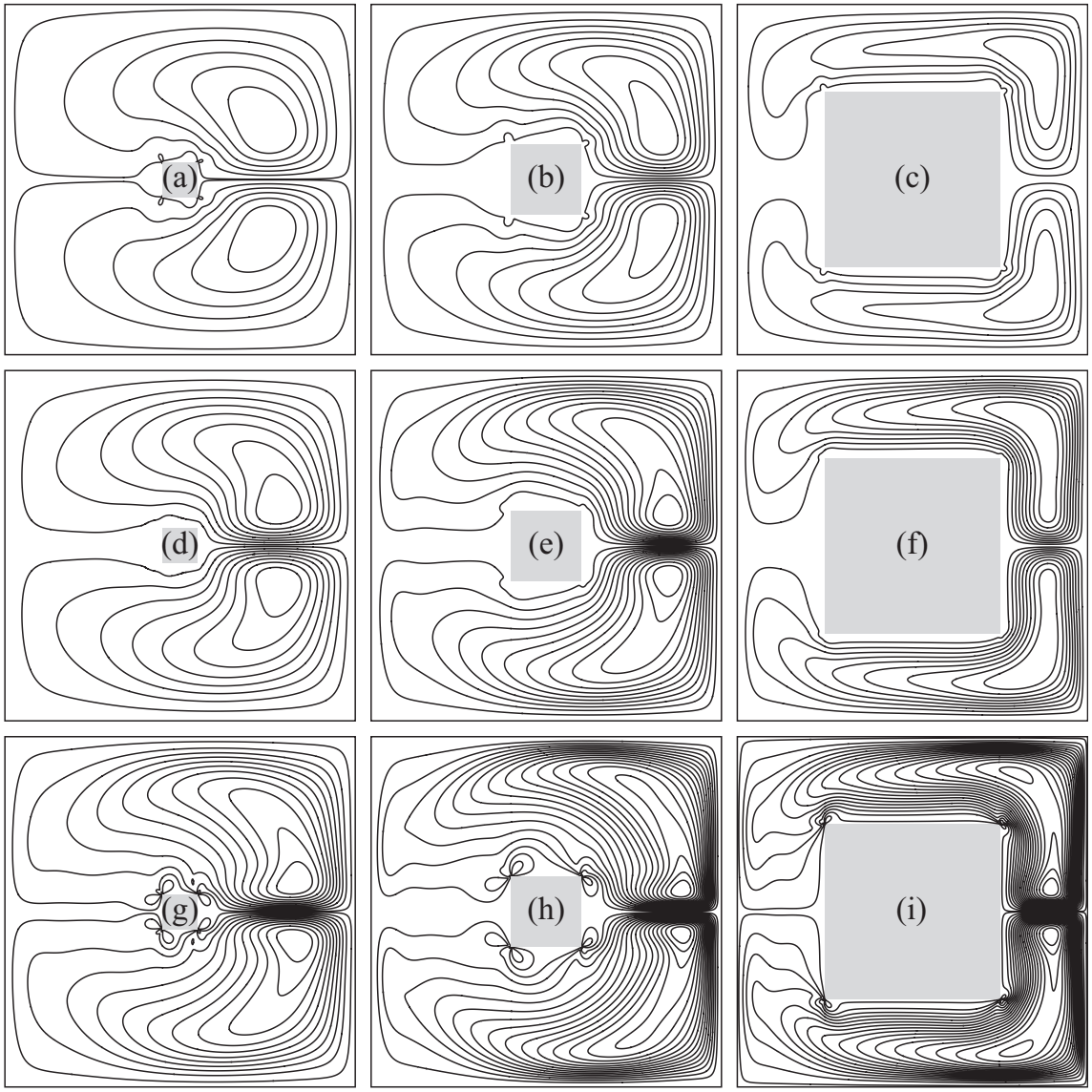

Fig. 3. Streamlines for permanent magnet size of d^* = 0.1, 0.2, and 0.5, for $Ra_m = 2.5 \times 10^8$ in (a)–(c); for $Ra_m = 1 \times 10^9$ in (d)–(f); and for $Ra_m = 5 \times 10^9$ in (g)–(i). The difference between two consecutive streamlines is $\Delta\psi^* = 2$.

sizes are summarized in Table 1. In comparison to the results obtained by a non-dimensional grid size of 0.0005, the results of average Nusselt number as well as the maximum stream function for the chosen grid systems yielded relative errors of less than 0.5% for the most stringent cases. These small grid sizes were found to be necessary to obtain accurate and stable solutions especially in high magnetic Rayleigh numbers. Furthermore, simulations for cases with $d^* > 0.5$ were carried out at finer grid sizes of 0.0005 for $Ra_m = 1 \times 10^9$ and 0.001 for $Ra_m = 2.5 \times 10^8$.

The validation of numerical code was checked by comparing the results of average Nusselt number in an air-filled cavity with the values reported by House et al. [63] and Merrikh and Lage [64]. As presented in Table 2, an empty cavity and cavities containing a single half-width solid block for two values of solid to fluid conductivity ratio (k_r) were considered. Another validation was performed for an air-filled cavity heated from below and cooled from above. Comparison of the isotherms with those given by Lee and Ha [65] for the cavity containing an adiabatic block of size $d^* = 1/3$ is presented in Fig. 2. The comparisons indicated that the results of the numerical code agree well with other published results.

Table 3
The minimum and maximum values of stream function in the upper half of the cavity for different magnetic Rayleigh number and permanent magnet size; for the lower half, the stream function has the same values with a negative sign.

	d^* = 0.1	d^* = 0.2	d^* = 0.5
$Ra_m = 2.5 \times 10^8$	−12.15/0.631	−16.88/0.676	−11.14/0.480
$Ra_m = 1 \times 10^9$	−16.82/0.145	−25.13/0.606	−19.57/0.456
$Ra_m = 5 \times 10^9$	−22.57/3.407	−35.76/3.688	−38.24/3.095

4. Results and discussion

The numerical results are presented for the various values of Magnetic Rayleigh number Ra_m and permanent magnet dimensionless size d^*. Also, the effect of temperature ratio of the isothermal walls on the flow and temperature fields is studied. The fixed values of $\beta_c = 60$ and Pr = 1000 are considered for the magnetization parameter and Prandtl number, respectively. These values are based on the typical ester oil-based ferrofluids containing iron

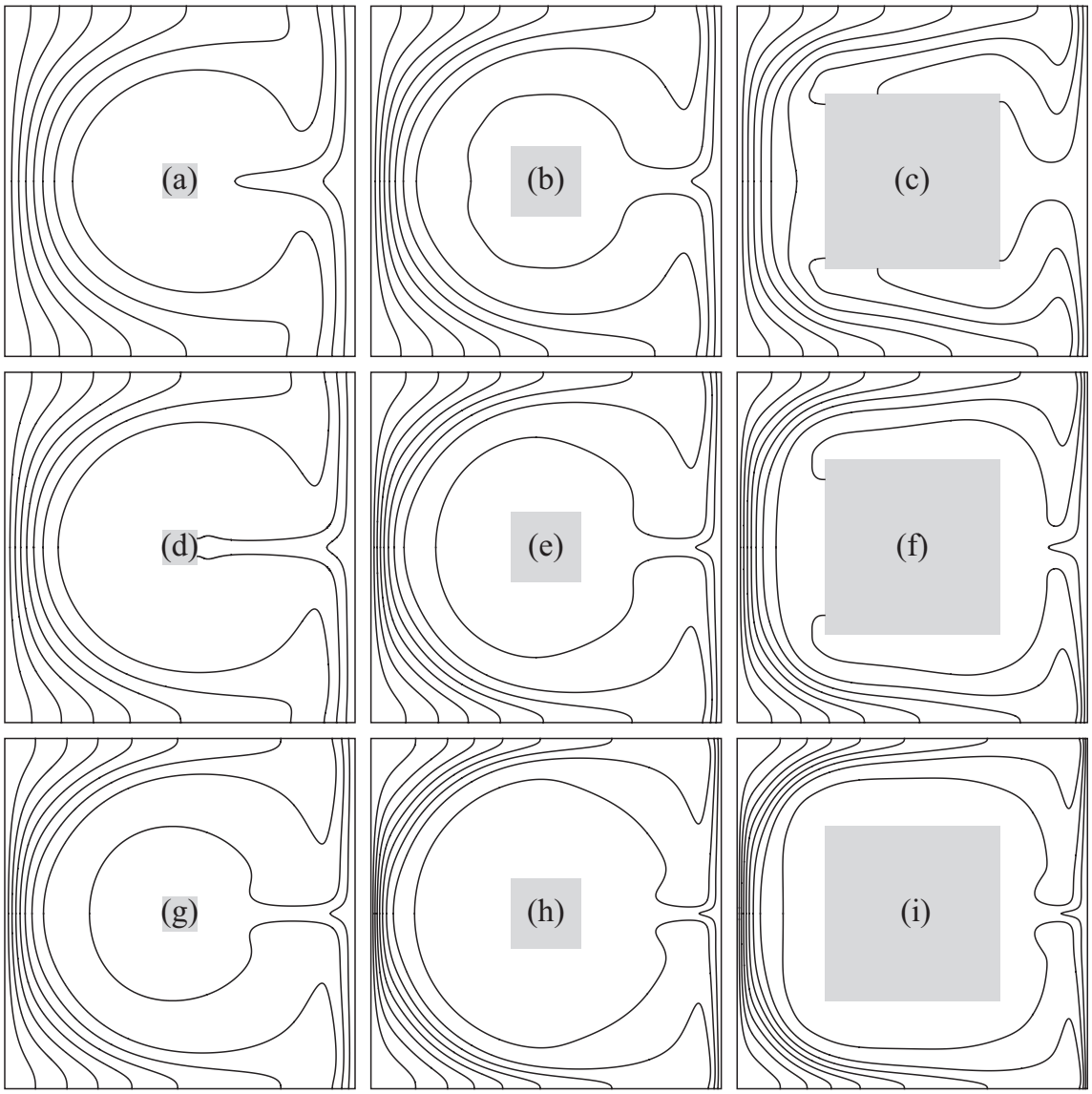

Fig. 4. Isotherms for permanent magnet size of d^* = 0.1, 0.2, and 0.5, for $Ra_m = 2.5 \times 10^8$ in (a)–(c); for $Ra_m = 1 \times 10^9$ in (d)–(f); and for $Ra_m = 5 \times 10^9$ in (g)–(i). The difference between two consecutive isotherms is $\Delta T^* = 0.1$.

particles of 10 nm mean diameter under the effect of NdFeB type permanent magnets at room temperature.

Fig. 3 shows the streamlines for magnetic Rayleigh numbers of 2.5×10^8, 1×10^9, and 5×10^9 for different permanent magnet sizes of $d^* = 0.1$, 0.2, and 0.5. The streamlines show two major circulations, a clockwise flow in the upper half of the cavity and a counterclockwise one in the lower half of the cavity. On the other hand, strong circulations are formed around the edges of permanent magnet surfaces having opposite directions (counterclockwise above the permanent magnet and clockwise below it). In Fig. 3, the intensity of circulations increases with the increase in magnetic Rayleigh number.

The corresponding minimum and maximum values of dimensionless stream function (defined as $\psi^* = \psi/\alpha$, where the wall value is set to zero) in the upper half of the cavity are listed in Table 3. For the lower half, the same values are obtained with a negative sign. There exist small stream values with opposite sign near the permanent magnet edges confirming the counterflow noted earlier. It is evident that the flow strength increases with the magnetic Rayleigh number. However, increasing the permanent magnet size has two contradictory effects on the flow field: (i) the increase in magnetic force and therefore increase in the fluid driving force, and (ii) the increase in blockage area and consequently increase of resistance in the flow. For example, at $Ra_m = 2.5 \times 10^8$, increasing the permanent magnet size from $d^* = 0.1$ to $d^* = 0.2$ reinforces the magnetic convection. In contrast, increasing the permanent magnet size from $d^* = 0.2$ to $d^* = 0.5$ suppresses the flow. This can also be seen for $Ra_m = 5 \times 10^9$ in Table 3. Increasing the magnetic Rayleigh number postpones the dominance of suppressing effect of increasing in the permanent magnet size.

As can be seen in Fig. 3, the flow is symmetric about the horizontal midline. But, there is no symmetric pattern about the vertical direction because the body force does not vary linearly with temperature. The ferrofluid magnetization expressed by Eq. (10) as a nonlinear function of the absolute temperature was found to be crucial for evaluating the Kelvin body force. The linear approximations for magnetization can be expressed as

$$M^* = \frac{\beta_c H^*}{3(1 + t_r T^*)} \tag{17a}$$

or

$$M^* = \frac{\beta_c H^*}{3}(1 - t_r T^*) \tag{17b}$$

in which the magnetic susceptibility is assumed to be independent of the applied magnetic field. The calculation of magnetization using Eq. (17) results in inaccurate values especially near the permanent magnet. For example, for the permanent magnet size $d^* = 0.2$, evaluating the magnetization using the linear approximation leads to a minimum error of 4% at the farthest point from the permanent magnet surface. For this case, the error exceeds more than 600% at the surface of the permanent magnet.

The isotherms for $Ra_m = 2.5 \times 10^8$, 1×10^9, and 5×10^9 for different permanent magnet sizes of $d^* = 0.1$, 0.2, and 0.5 are presented in Fig. 4. As can be seen, the temperature gradient near the isothermal walls increases with the increase in Ra_m. Consequently, increasing the magnetic Rayleigh number results in a more uniform temperature distribution near the permanent magnet due to increase in the magnetic convective flow.

Variations of the local Nusselt number along the left and right walls at $Ra_m = 1 \times 10^9$ for different permanent magnet sizes are shown in Fig. 5. The values of Nusselt number on the right wall show minimums at the center induced by the effect of strong flow at the center of right wall. This is due to high magnetic forces generated for the low temperature ferrofluid by the permanent magnet. Furthermore, local maximums are observed near the right-side corners, influenced by the weakened main circulations. In contrast, as a result of relatively stagnant high-temperature ferrofluid near the left wall (see Fig. 3), the values of Nusselt number show maximums at the wall center on the left side.

The results of average Nusselt number for the above mentioned cases are reported in Table 4. For $Ra_m = 0$, the average Nusselt number is below 1. That is because the equivalent conductivity of the cavity in this case is lower than the ferrofluid conductivity due to the presence of an isolated solid block [66]. For the presented data, the blockage resistance of increasing the permanent magnet size is more pronounced at $Ra_m = 2.5 \times 10^8$. However, for these cases, the Nusselt number increased with the increase in permanent magnet size. The magnetic Rayleigh number always has an increasing effect on the heat transfer rate.

The presented results reveal that there exists an optimum size for the permanent magnet for a fixed set of other dimensionless parameters values. The heat transfer rate for different permanent magnet sizes at $Ra_m = 2.5 \times 10^8$ and 1×10^9 is evaluated, as presented in Fig. 6. The Nusselt number increases from unity as the permanent magnet size increases from $d^* = 0$ (an empty cavity) to a maximum value at a specific d^* depending on the physical parameters (Ra_m, Pr, t_r, and β_c). After that, the Nusselt number decreases with increasing the permanent magnet size. Theoretically, the optimal value of non-dimensional permanent magnet size increases from 0 to 1 by increasing the magnetic Rayleigh number from 0 to infinity. The optimal values of $d^* = 0.35$ and $d^* = 0.45$ (accuracy ±0.05) are found for $Ra_m = 2.5 \times 10^8$ and 1×10^9, respectively.

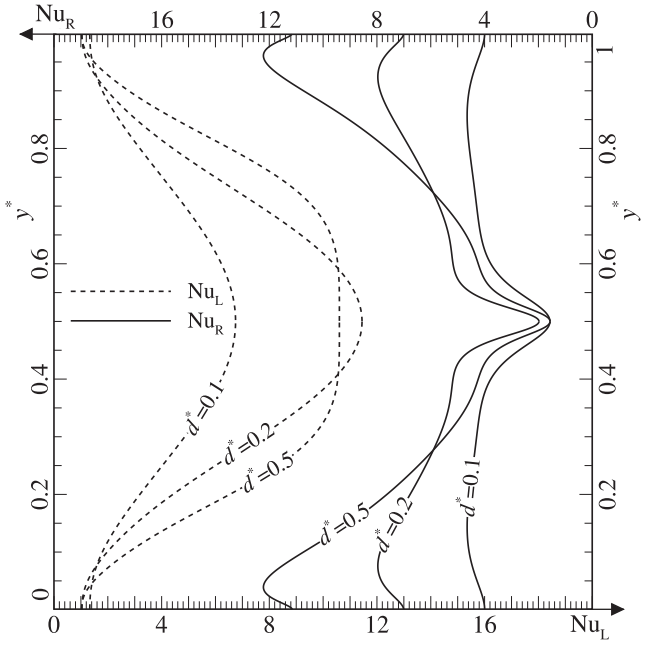

Fig. 5. Local Nusselt number along the isothermal walls for different permanent magnet size at $Ra_m = 1 \times 10^9$.

Table 4
The average Nusselt number for different magnetic Rayleigh number and permanent magnet size.

	$d^* = 0.1$	$d^* = 0.2$	$d^* = 0.5$
$Ra_m = 0$	0.978	0.916	0.577
$Ra_m = 2.5 \times 10^8$	3.202	4.667	4.684
$Ra_m = 1 \times 10^9$	4.021	6.134	7.051
$Ra_m = 5 \times 10^9$	5.354	8.437	10.06

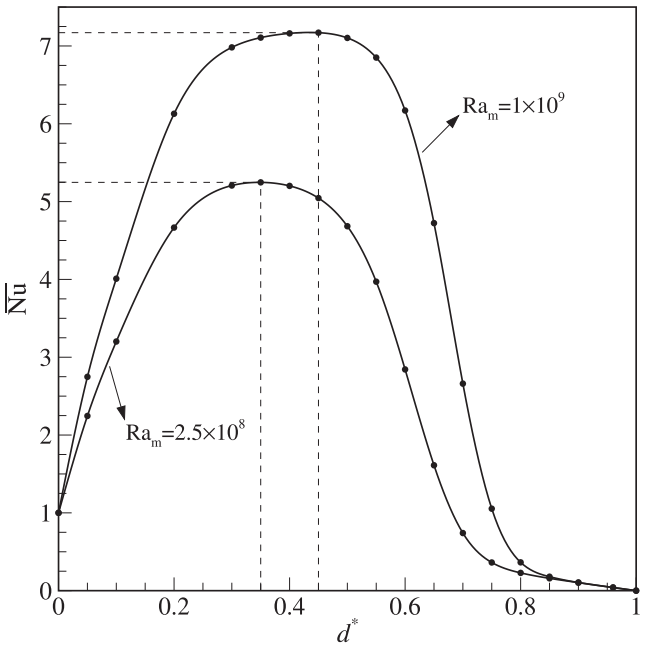

Fig. 6. The average Nusselt number versus permanent magnet size; there is an optimum permanent magnet size for each case.

It is of practical interest to study the effect of walls temperature ratio (t_r) on the flow and temperature fields. Figs. 7 and 8 present the streamlines and isotherms, respectively, for different magnetic Rayleigh numbers for a cavity with a permanent magnet of size $d^* = 0.5$ and temperature ratio of $t_r = 0.2$. In these figures, the dashed lines indicate the corresponding results for $t_r = 0.1$. Based on Eq. (10), increasing the temperature ratio reduces the magnetization coefficient β, but, increases its range. For $\beta_c = 60$ and $t_r = 0.1$, β varies between 54.5 and 60. This coefficient varies between 50 and 60 for $t_r = 0.2$. Thus, increasing the temperature ratio increases the magnetization *differences* in the ferrofluid and the magnetic convection strengthen accordingly. By increasing the temperature ratio from 0.1 to 0.2, the Nusselt number increased by 26, 17, and 15 percent for $Ra_m = 2.5 \times 10^8$, 1×10^9, and 5×10^9, respectively.

The present configuration has potential applications for cooling devices. The studied magnetic Rayleigh numbers are for 1–5 cm square cavities filled with the oil-based ferrofluids. The larger cavities, especially filled with the water-based ferrofluids, lead to higher magnetic Rayleigh numbers. Consequently, stronger flows and hence more heat transfer rates will be generated where turbulence develops and laminar flow is not valid. Recently, a study on determination of the critical Rayleigh number for the transition from conduction to thermomagnetic convection is conducted [67]. In contrast, experimental and numerical studies of turbulent

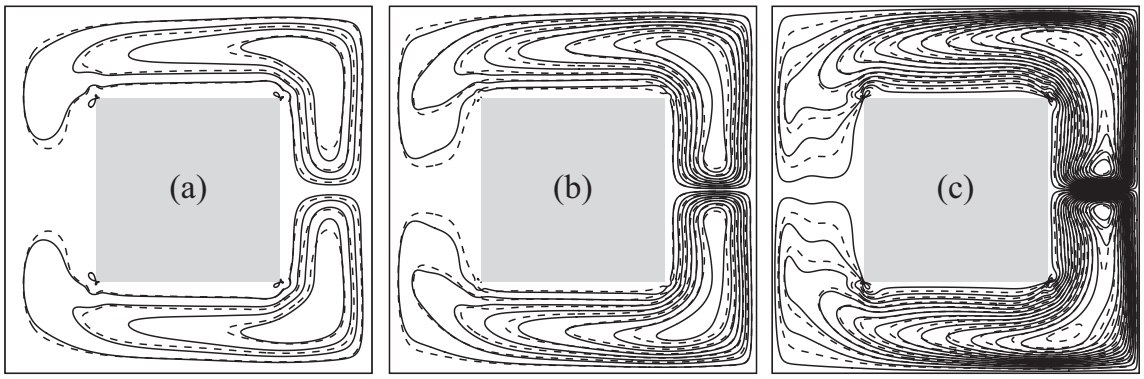

Fig. 7. Streamlines for $d^* = 0.5$ and $t_r = 0.2$, at (a) $Ra_m = 2.5 \times 10^8$, (b) $Ra_m = 1 \times 10^9$ and (c) $Ra_m = 5 \times 10^9$; the dashed lines indicate the streamlines for $t_r = 0.1$. The difference between two consecutive streamlines is $\psi^* = 2$.

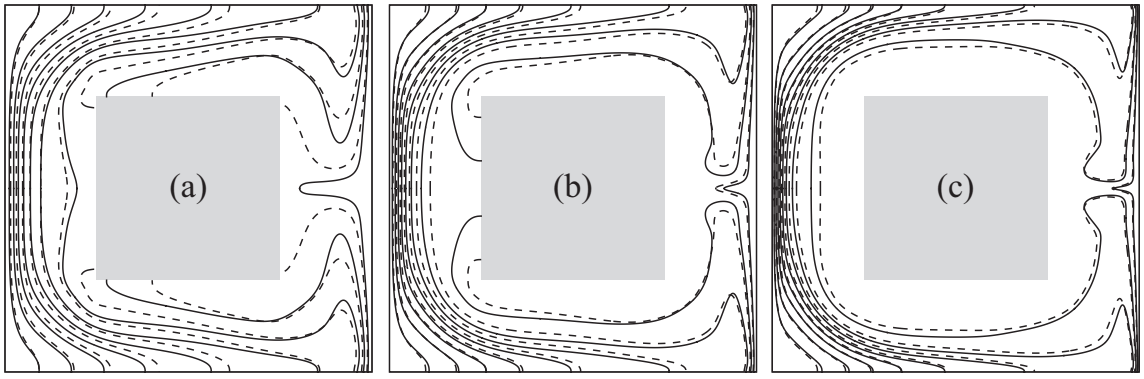

Fig. 8. Isotherms for $d^* = 0.5$ and $t_r = 0.2$, at (a) $Ra_m = 2.5 \times 10^8$, (b) $Ra_m = 1 \times 10^9$ and (c) $Ra_m = 5 \times 10^9$; the dashed lines indicate the corresponding isotherms for $t_r = 0.1$. The difference between two consecutive isotherms is $\Delta T^* = 0.1$.

velocity and temperature fields for high magnetic Rayleigh number thermomagnetic convection are of interest as well.

5. Conclusions

The flow and heat transfer characteristics of magnetic convection ferrofluid flow in a square cavity was studied. A square permanent magnet inserted into the center of the cavity had induced the Kelvin body force to the ferrofluid. The thermal buoyancy flow was ignored due to non-gravity condition on the plane of the cavity. This configuration has potential applications for heat removal, particularly in small-scale cooling devices. The governing equations were solved numerically using the finite volume method. The simulations were carried out for the various magnetic Rayleigh number, permanent magnet size, and temperature ratio between the cold and hot walls, while the physical parameters of magnetization parameter β_c and Prandtl number Pr were kept fixed. The results indicated the following points:

- The increase in permanent magnet size has two contrary effects on the flow field: the strengthening in the ferrofluid driving force due to the increased magnetic field, and the increase in the resistance to the fluid flow by the geometrical influence. For small sizes, the positive effect is prevailing. However, the suppressing effect will be dominant if the size is excessively increased. The dominance of the negative effect is postponed by increasing the magnetic Rayleigh number. The heat transfer rate for different permanent magnet sizes was evaluated and the optimum size for the permanent magnet was found.
- The analysis of the effect of the temperature ratio on the heat transfer rate indicates that increasing the temperature ratio increases the magnetization differences in the ferrofluid. Thus, the strength of magnetic convection and the heat transfer rate increase.

Acknowledgements

We would like to express our gratitude to the Deputy for Research and Technology of Sharif University of Technology for supporting this research study. The first author also wishes to thank the Iranian National Elite Foundation for the support of his postdoctoral program.

References

[1] R.E. Rosensweig, Ferrohydrodynamics, Courier Corporation, 2013.
[2] R.E. Rosensweig, Y. Hirota, S. Tsuda, K. Raj, Study of audio speakers containing ferrofluid, J. Phys. Condens. Mat. 20 (2008), 204147–1 5.
[3] M. Pinho, J.M. Génevaux, N. Dauchez, B. Brouard, P. Collas, H. Mézière, Damping induced by ferrofluid seals in ironless loudspeaker, J. Magn. Magn. Mater. 356 (2014) 125–130.
[4] M. De Volder, D. Reynaerts, Development of a hybrid ferrofluid seal technology for miniature pneumatic and hydraulic actuators, Sens. Actuators, A 152 (2009) 234–240.
[5] P. Kuzhir, Free boundary of lubricant film in ferrofluid journal bearings, Tribol. Int. 41 (2008) 256–268.
[6] H. Ruican, L. Huagang, G. Wen, Z. Na, H. Ruixiao, Research experiments on pressure-difference sensors with ferrofluid, J. Magn. Magn. Mater. 416 (2016) 231–235.
[7] A. Amirabadizadeh, Z. Lotfollahi, A. Zelati, Giant magnetoimpedance effect of Co68.15 Fe4.35 Si12.5 B15 amorphous wire in the presence of magnetite ferrofluid, J. Magn. Magn. Mater. 415 (2016) 102–105.
[8] B. Andò, S. Baglio, A. Beninato, A ferrofluid inclinometer with a time domain readout strategy, Sens. Actuators, A 202 (2013) 57–63.
[9] B. Andò, S. Baglio, A. Beninato, A flow sensor exploiting magnetic fluids, Sens. Actuators, A 189 (2013) 17–23.
[10] S. Pal, A. Datta, S. Sen, A. Mukhopdhyay, K. Bandopadhyay, R. Ganguly, Characterization of a ferrofluid-based thermomagnetic pump for microfluidic applications, J. Magn. Magn. Mater. 323 (2011) 2701–2709.
[11] E. Aursand, M.A. Gjennestad, K.Y. Lervåg, H. Lund, Potential of enhancing a natural convection loop with a thermomagnetically pumped ferrofluid, J. Magn. Magn. Mater. 417 (2016) 148–159.
[12] M. Taslimifar, M. Mohammadi, H. Afshin, M.H. Saidi, M.B. Shafii, Overall thermal performance of ferrofluidic open loop pulsating heat pipes: An experimental approach, Int. J. Therm. Sci. 65 (2013) 234–241.
[13] M. Mohammadi, M. Taslimifar, M.H. Saidi, M.B. Shafii, H. Afshin, S.K. Hannani, Ferrofluidic open loop pulsating heat pipes: efficient candidates for thermal management of electronics, Exp. Heat Transfer 27 (2014) 296–312.
[14] L. Mao, H. Koser, Ferrohydrodynamic pumping in spatially traveling sinusoidally time-varying magnetic fields, J. Magn. Magn. Mater. 289 (2005) 199–202.
[15] L. Mao, S. Elborai, X. He, M. Zahn, H. Koser, Direct observation of closed-loop ferrohydrodynamic pumping under traveling magnetic fields, Phys. Rev. B 84 (2011), 104431–1 7.
[16] M. Ashouri, M.B. Shafii, A. Moosavi, Theoretical and experimental studies of a magnetically actuated valveless micropump, J. Micromech. Microeng. (2017), in press.
[17] M. Ashouri, M.B. Shafii, A. Moosavi, Diffuser miniature pump with an extra ferrofluidic valve, Microfluid. Nanofluid. 19 (2015) 1235–1244.
[18] M. Ashouri, M.B. Shafii, A. Moosavi, H. Amiri Hezave, A novel revolving piston minipump, Sens. Actuators, A 218 (2015) 237–244.
[19] G. Kitenbergs, K. Ērglis, R. Perzynski, A. Cēbers, Magnetic particle mixing with magnetic micro-convection for microfluidics, J. Magn. Magn. Mater. 380 (2015) 227–230.
[20] N. Azimi, M. Rahimi, Magnetic nanoparticles stimulation to enhance liquid-liquid two-phase mass transfer under static and rotating magnetic fields, J. Magn. Magn. Mater. 422 (2017) 188–196.
[21] N.-T. Nguyen, G. Zhu, Y.-C. Chua, V.-N. Phan, S.-H. Tan, Magnetowetting and sliding motion of a sessile ferrofluid droplet in the presence of a permanent magnet, Langmuir 26 (2010) 12553–12559.
[22] C. Rigoni, M. Pierno, G. Mistura, D. Talbot, R. Massart, J.-C. Bacri, A. Abou-Hassan, Static magnetowetting of ferrofluid drops, Langmuir 32 (2016) 7639–7646.
[23] S. Tokura, M. Hara, N. Kawaguchi, N. Amemiya, Contactless magnetic manipulation of magnetic particles in a fluid, J. Magn. Magn. Mater. 411 (2016) 68–78.
[24] T. Zhu, R. Cheng, G.R. Sheppard, J. Locklin, L. Mao, Magnetic-field-assisted fabrication and manipulation of nonspherical polymer particles in ferrofluid-based droplet microfluidics, Langmuir 31 (2015) 8531–8534.
[25] N.T. Nguyen, Micro-magnetofluidics: interactions between magnetism and fluid flow on the microscale, Microfluid. Nanofluid. 12 (2012) 1–16.
[26] I. Torres-Díaz, C. Rinaldi, Recent progress in ferrofluids research: novel applications of magnetically controllable and tunable fluids, Soft Matter 10 (2014) 8584–8602.
[27] R.-J. Yang, H.-H. Hou, Y.-N. Wang, L.-M. Fu, Micro-magnetofluidics in microfluidic systems: a review, Sens. Actuators, B 224 (2016) 1–15.
[28] M. Bahiraei, M. Hangi, Flow and heat transfer characteristics of magnetic nanofluids: a review, J. Magn. Magn. Mater. 374 (2015) 125–138.
[29] A.E. Kabeel, E.M.S. El-Said, S.A. Dafea, A review of magnetic field effects on flow and heat transfer in liquids: present status and future potential for studies and applications, Renewable Sustainable Energy Rev. 45 (2015) 830–837.
[30] R. Touihri, A. El Gallaf, D. Henry, H. Ben Hadid, Instabilities in a cylindrical cavity heated from below with a free surface. II. Effect of a horizontal magnetic field, Phys. Rev. E 84 (2011) 056303-1–056303-13.
[31] P. Mostaghimi, M. Ashouri, B. Ebrahimi, Hydrodynamics of fingering instability in the presence of a magnetic field, Fluid Dyn. Res. 48 (2016) 055504–055519.
[32] D. Zablotsky, A. Mezulis, E. Blums, Surface cooling based on the thermomagnetic convection: numerical simulation and experiment, Int. J. Heat Mass Transfer 52 (2009) 5302–5308.
[33] A. Bozhko, G. Putin, Thermomagnetic convection as a tool for heat and mass transfer control in nanosize materials under microgravity conditions, Microgravity Sci. Technol. 21 (2008) 89–93.
[34] I. Nkurikiyimfura, Y. Wang, Z. Pan, Heat transfer enhancement by magnetic nanofluids—a review, Renewable Sustainable Energy Rev. 21 (2013) 548–561.
[35] E. Blums, A. Mezulis, G. Kronkalns, Magnetoconvective heat transfer from a cylinder under the influence of a nonuniform magnetic field, J. Phys. Condens. Mater. 20 (2008), 204128–1 5.
[36] D. Zablockis, V. Frishfelds, E. Blums, Numerical investigation of thermomagnetic convection in a heated cylinder under the magnetic field of a solenoid, J. Phys. Condens. Mater. 20 (2008), 204134–1 5.
[37] R. Ganguly, S. Sen, I.K. Puri, Heat transfer augmentation using a magnetic fluid under the influence of a line dipole, J. Magn. Magn. Mater. 271 (2004) 63–73.
[38] H. Aminfar, M. Mohammadpourfard, S. Ahangar Zonouzi, Numerical study of the ferrofluid flow and heat transfer through a rectangular duct in the presence of a non-uniform transverse magnetic field, J. Magn. Magn. Mater. 327 (2013) 31–42.
[39] M. Lajvardi, J. Moghimi-Rad, I. Hadi, A. Gavili, T. Dallali Isfahani, F. Zabihi, J. Sabbaghzadeh, Experimental investigation for enhanced ferrofluid heat transfer under magnetic field effect, J. Magn. Magn. Mater. 322 (2010) 3508–3513.
[40] F. Selimefendigil, H.F. Öztop, Forced convection of ferrofluids in a vented cavity with a rotating cylinder, Int. J. Therm. Sci. 86 (2014) 258–275.
[41] C.Y. Wen, W.P. Su, Natural convection of magnetic fluid in a rectangular Hele-Shaw cell, J. Magn. Magn. Mater. 289 (2005) 299–302.

[42] A. Jafari, T. Tynjälä, S.M. Mousavi, P. Sarkomaa, CFD simulation and evaluation of controllable parameters effect on thermomagnetic convection in ferrofluids using Taguchi technique, Comput. Fluids 37 (2008) 1344–1353.
[43] A. Jafari, T. Tynjälä, S.M. Mousavi, P. Sarkomaa, Simulation of heat transfer in a ferrofluid using computational fluid dynamics technique, Int. J. Heat Fluid Flow 29 (2008) 1197–1202.
[44] M. Sheikholeslami, D.D. Ganji, Ferrohydrodynamic and magnetohydrodynamic effects on ferrofluid flow and convective heat transfer, Energy 75 (2014) 400–410.
[45] M. Sheikholeslami, D.D. Ganji, M.M. Rashidi, Ferrofluid flow and heat transfer in a semi annulus enclosure in the presence of magnetic source considering thermal radiation, J. Taiwan Inst. Chem. Eng. 47 (2015) 6–17.
[46] F. Selimefendigil, H.F. Öztop, Numerical study and POD-based prediction of natural convection in a ferrofluids-filled triangular cavity with generalized neural networks, Numer. Heat Transfer A 67 (2015) 1136–1161.
[47] H. Yamaguchi, X.-D. Niu, X.-R. Zhang, K. Yoshikawa, Experimental and numerical investigation of natural convection of magnetic fluids in a cubic cavity, J. Magn. Magn. Mater. 321 (2009) 3665–3670.
[48] H. Yamaguchi, X.-R. Zhang, X.-D. Niu, K. Yoshikawa, Thermomagnetic natural convection of thermo-sensitive magnetic fluids in cubic cavity with heat generating object inside, J. Magn. Magn. Mater. 322 (2010) 698–704.
[49] H.L.G. Couto, N.B. Marcelino, F.R. Cunha, A study on magnetic convection in a narrow rectangular cavity, J. Magnetohydrodynamics 43 (2007) 421–428.
[50] C. Tangthieng, B.A. Finlayson, J. Maulbetsch, T. Cader, Heat transfer enhancement in ferrofluids subjected to steady magnetic fields, J. Magn. Magn. Mater. 201 (1999) 252–255.
[51] H. Yamaguchi, I. Kobori, Y. Uehata, Heat transfer in natural convection of magnetic fluids, J. Thermophys. Heat Transfer 13 (1999) 501–507.
[52] H. Yamaguchi, I. Kobori, Y. Uehata, K. Shimada, Natural convection of magnetic fluid in a rectangular box, J. Magn. Magn. Mater. 201 (1999) 264–267.
[53] A. Mukhopadhyay, R. Ganguly, S. Sen, I.K. Puri, A scaling analysis to characterize thermomagnetic convection, Int. J. Heat Mass Transfer 48 (2005) 3485–3492.
[54] M. Ashouri, B. Ebrahimi, M.B. Shafii, M.H. Saidi, M.S. Saidi, Correlation for Nusselt number in pure magnetic convection ferrofluid flow in a square cavity by a numerical investigation, J. Magn. Magn. Mater. 322 (2010) 3607–3613.
[55] M.S. Krakov, I.V. Nikiforov, To the influence of uniform magnetic field on thermomagnetic convection in square cavity, J. Magn. Magn. Mater. 252 (2002) 209–211.
[56] H. Yamaguchi, Z. Zhang, S. Shuchi, K. Shimada, Heat transfer characteristics of magnetic fluid in a partitioned rectangular box, J. Magn. Magn. Mater. 252 (2002) 203–205.
[57] M.S. Krakov, I.V. Nikiforov, Thermomagnetic convection in a porous enclosure in the presence of outer uniform magnetic field, J. Magn. Magn. Mater. 289 (2005) 278–280.
[58] F. Selimefendigil, H.F. Öztop, K. Al-Salem, Natural convection of ferrofluids in partially heated square enclosures, J. Magn. Magn. Mater. 372 (2014) 122–133.
[59] F. Selimefendigil, H.F. Öztop, Numerical study of natural convection in a ferrofluid-filled corrugated cavity with internal heat generation, J. Heat Transfer 138 (2016), 122501–1 14.
[60] J.L. Neuringer, R.E. Rosensweig, Ferrohydrodynamics, Phys. Fluids 7 (1964) 1927–1937.
[61] S. Odenbach, Magnetoviscous Effects in Ferrofluids, Springer, Berlin Heidelberg, 2002.
[62] S.V. Patankar, Numerical Heat Transfer and Fluid Flow, Hemisphere Publishing Corp, Washington, DC, 1980.
[63] J.M. House, C. Beckermann, T.F. Smith, Effect of a centered conducting body on natural convection heat transfer in an enclosure, Numer. Heat Transfer A 18 (1990) 213–225.
[64] A.A. Merrikh, J.L. Lage, Natural convection in an enclosure with disconnected and conducting solid blocks, Int. J. Heat Mass Transfer 48 (2005) 1361–1372.
[65] J.R. Lee, M.Y. Ha, A numerical study of natural convection in a horizontal enclosure with a conducting body, Int. J. Heat Mass Transfer 48 (2005) 3308–3318.
[66] M. Ashouri, M.B. Shafii, H. Rajabi Kokande, MHD natural convection flow in cavities filled with square solid blocks, Int. J. Numer. Methods Heat Fluid Flow 24 (2014) 1813–1830.
[67] M. Heckert, L. Sprenger, A. Lange, S. Odenbach, Experimental determination of the critical Rayleigh number for thermomagnetic convection with focus on fluid composition, J. Magn. Magn. Mater. 381 (2015) 337–343.